

## Algorithm for Object Grasp Detection

<sup>1</sup>Robinson Jimenez Moreno, <sup>1</sup>Mauricio Mauledoux and <sup>2</sup>B. Javier Martinez  
<sup>1</sup>Faculty of Engineering, Nueva Granada Military University, Bogota, Colombia  
<sup>2</sup>University of Llanos, Meta, Colombia

---

**Abstract:** The following study presents the development of an algorithm for the detection of the grasp point for an object using gripper. The algorithm receives as input a white background image of the object to be grasped as well as the dimensions of the gripper in pixels. Also, the grip parameters are defined that will allow to discard those sections of the object that the gripper cannot take, parameters such as the minimum and maximum thickness of the admissible grip section in order to prevent the fit between the gripper and the object section being too loose or too tight, the thickness of the tips of the gripper is taken as a parameter to avoid collisions and the maximum degree of inclination between the object section and the surface of the gripper, so that, in the adjustment between both, the object does not move too much. It was possible to obtain an algorithm that allows to achieve a suitable point for taking objects in all cases evaluated, however, because of the distance from the center of gravity of the object it requires a higher strength for its grasp.

**Key words:** Robot grasp detection, object recognition, image processing, gripper, parameter, algorithm

---

### INTRODUCTION

Currently, one of the great challenges of robotics is to give a robot the ability to autonomously manipulate different types of objects in an uncontrolled environment, using solutions that can be applied in real time and that allow to manipulate objects of different physical characteristics not bounded, like scissors, for example. In Yon (2016), it is proposed an algorithm that allows to determine the grip for objects with a certain axial symmetry where a cloud of points is filtered and segmented, several points of grip are determined, a score is assigned to each one and finally, the winner is chosen.

On the other hand by Martin (2015) they developed, under a ROS environment (Robot Operating System), an object grab system for an industrial robot, defining two priority selection parameters for the grip: the distance between the gripper and the desired object and the quality of the grip which is based on the contact surface between the gripper and the element, choosing the one with the largest contact area for gripping precision, force or for fastening objects with low friction.

In the case presented by Fernandez *et al.* (2003) an algorithm of grasp detection by pattern learning provided by the user is proposed through teleoperation, making use of decision trees where in a first stage, all possible grip points are obtained and in the second those that match the geometry of the gripper are sought in order to finally choose the optimum grip.

There are also developments of grasp detection algorithms using convolutional neural networks and machine vision using the 3D camera of Microsoft Kinect as presented by Trottier *et al.* (2016). In other cases such as that proposed by Jain and Argall (2016) and Cruz they are obtained geometric approximations of the detected objects to determine the grip position or from a cloud of points all possible grips are obtained and from them a classification of good and bad grips by means of convolutional neural networks as by Gualtieri *et al.* (2016).

By Redmon and Angelova (2015), a real-time classification and detection algorithm was proposed using a window that covers each frame of a video and convolutional neural networks for the grasp detection. In a similar way by Wang *et al.* (2016) an algorithm of object detection was proposed that allows to identify the elements that can be held by the gripper and on them a convolutional neural network is applied to select the final grip position.

By Sun *et al.* (2015) an algorithm of grasp detection was developed by means of extreme machine learning where three successive modules were used: the first detects the candidate objects for the grasp, the second estimates the orientation of the object and the third one detects the grasp mode.

Next, the development of a grasp detection algorithm for objects with different geometries that can be conditioned to any particular application, varying parameters such as the dimensions of the gripper, the

minimum degree of rotation of the gripper and the degree of maximum inclination between the object and the gripper that is supported in the application. This algorithm is characterized by having the ability to determine the grip for different families of elements based on geometric characteristics such as the thickness in the grip section and the contact surface between the object and the gripper in order to increase friction between the elements in addition to allowing adjustment of their parameters to be conditioned to a particular application.

### MATERIALS AND METHODS

**Basic operation of the algorithm:** The developed algorithm allows to set the gripping position of a desired object. Through, image processing of the scene on which the objects are found it is possible to discriminate, each one by difference of the background and of tonality. Discriminated the object, the points of closest grip to its centroid are sought. In the development of the algorithm white background images were evaluated with objects of different geometries and the X and Y

positions of the grasp point and the orientation with which the gripper should take the object were obtained.

Figure 1 shows the basic structure of the algorithm by means of a flowchart from the moment the image is entered to the output of the coordinates and the orientation of the grip for a gripper type gripper where from said flowchart, 19 base points of the algorithm are recognized.

Steps 1-3 of Fig. 1 are responsible for the initialization of the program in which the image is captured and the segmentation of the object through a thresholding process. In steps 4-7, sections of the input image are cut in different positions and orientations to search for possible grip points in each of them. Steps 8 through 12 evaluate each cut and save only those that meet the conditions in steps 8 through 11. Steps 13 and 14 are executed only when no grip is found throughout the image. In steps 15-17 all the grips saved in step 12 are selected to choose one of them as the winning grasp point and in steps 18 and 19 the results are shown. Each of the steps in the flowchart of Fig. 1 will be explained.

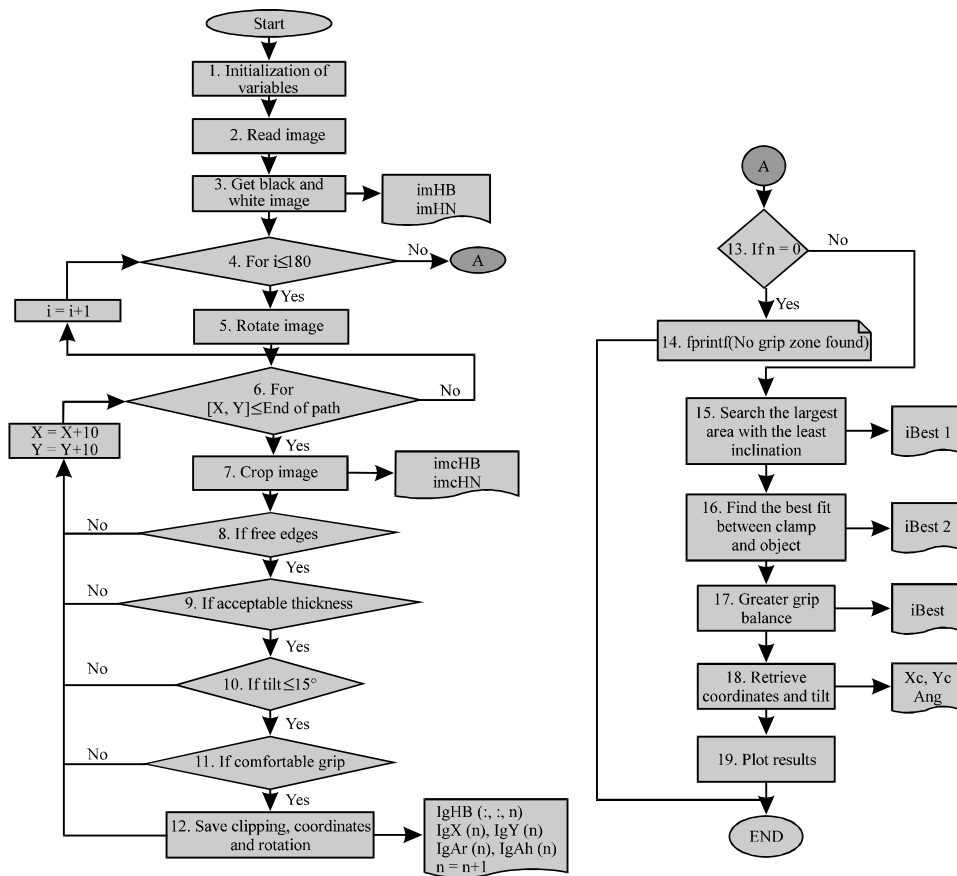


Fig. 1: Flow chart

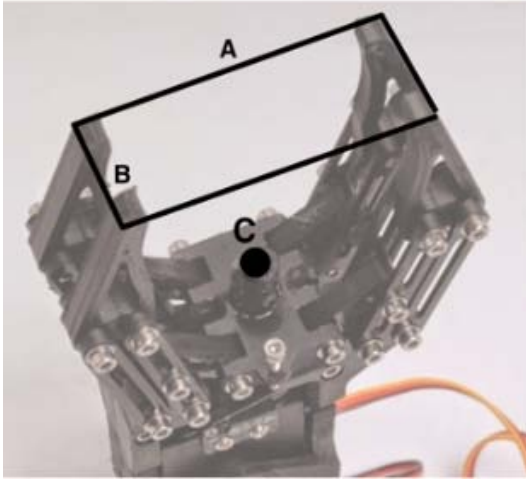


Fig. 2: Gripper dimensions

**Program initialization:** In step 1, the variables of the algorithm are initialized such as the dimensions of the gripper (opening and width of the tips) it is determined how many degrees the image is rotated to evaluate grip points in different orientations, the maximum and minimum thickness of the grip section of the object is established and the amount of free pixels that must exist between the gripping zone and the tips of the gripper.

Figure 2 shows the width and opening dimensions of the gripper that must be initialized in the algorithm in order to know the space occupied by the gripper inside the work area and avoid collisions between the elements when the gripper proceeds to make the grasp and they are also used to define the maximum opening of the gripper when selecting the grasp point.

The dimension A represents the opening of the gripper plus the thickness of the tips. Dimension B represents the width of the gripper and the point C represents the center of the gripper corresponding to the positions  $X_c$  and  $Y_c$  that determine the grasp final position.

In step 2, the image is taken from the work area which is resized to  $220 \times 220$  pixels. In step 3, the process of thresholding and binarization of the image is carried out where a color space conversion of the original image in RGB into grayscale is made and finally to black and white in such a way that the background of the image is completely black and only the object on it, remains white (imHB) as seen in Fig. 3a. Following this, the binarized image is taken and the intensity of its pixels is exchanged to obtain a second image (imHN) with a completely white background and the object in black as shown in Fig. 3b. The threshold was defined in the algorithm as 0.9 because

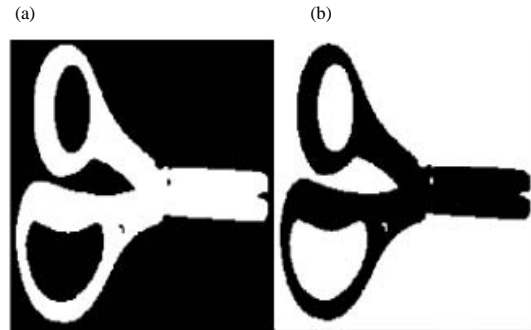


Fig. 3: a, b) Binarized image

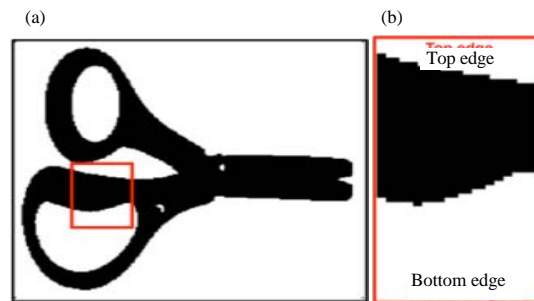


Fig. 4: a, b) ImcHN cut with a possible grasp

all the images tested were white background, so, it was not necessary to consider light changes under a controlled testing environment.

**Image processing:** On each of the binarized images (imHN and imHB), a box with dimensions A and B, initialized in step 1 was moved where its initial position is in the upper left corner of the image that coincides with the upper left corner of the box and moves down a position equivalent to 10 pixels in search of possible grips. This box represents the area occupied by the gripper over the space when looking for the object of work, so that, from this box can be estimated where there is a possible grip and where the gripper, definitely cannot hold the object.

In each position of the frame, the section of the image underneath is trimmed, both for the imcHN image (where the cut is saved imcHN) and for the imcHB (where the cut is saved imcHB). Each cutout is independently evaluated by passing the conditionals of steps 8-11 of the flowchart of Fig. 1 to determine whether it is a possible grasp or not. When it reaches step 12 of Fig. 1 or does not meet any of the conditionals in steps 8 through 11, the box is moved down one position to evaluate the next cut.

In Fig. 4b, a possible grasp for the imHN image can be observed where the image section which is cut from the

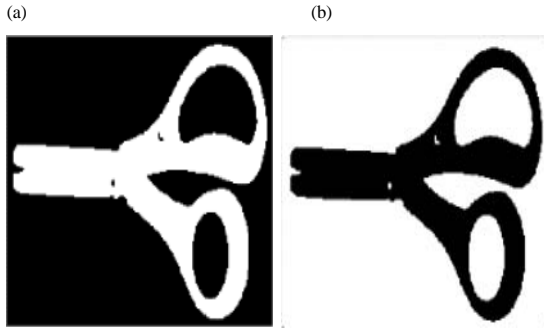


Fig. 5: Image inverted; a) imHB and b) imHN

box in Fig. 4a is stored. In the “Selection of possible grasp” section, each of the conditionals of steps 8-11 of Fig. 1 is explained in detail for the selection of a possible grasp point.

Once the descending movement finishes and reaches the bottom of the image it returns to its initial position but 10 pixels shifts to the right and then moves down again to draw new cuts and in this way successively, increasing its horizontal displacement every 10 pixels until reach the lower right corner of the image with all possible stored grips.

The number of pixels that the box moves in the frame was selected as 10 to speed up the grasp search process considering the dimensions of the input image and to avoid holding possible very close grips that increase the amount of data to be stored.

When the frame that traverses the image ends the path, i.e., its lower right corner coincides with the lower right corner of the binarized image it returns to steps 4 and 5 of Fig. 1 to generate a rotation in the image and thus, return to steps 6 and 7 to capture new clippings but with the image rotated at a certain angle.

This process allows to find new grips with different orientations of the gripper and is repeated until the image is rotated a total of 180°. When the image has been rotated a total of 180° it means that it has been completely turned (Fig. 5) and therefore, all possible grips on the object have been evaluated, since, to continue with the rotation will only cause the collected grips to be repeated but in reverse positions as shown in Fig. 6.

The cutouts (imcHN and imcHB) of both binarized images are obtained in order to apply all the selection criteria found in steps 8-11. To apply these criteria it is necessary to know aspects of the image as the number of white pixels to the upper and lower edges of the imcHN cutout (Fig. 6) and the number of white pixels in the imcHB cutout to know the width of the captured object within the cutout.

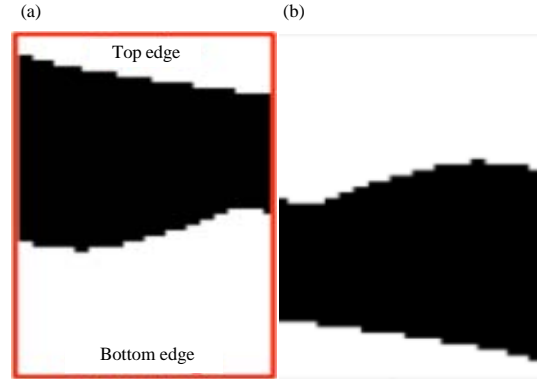


Fig. 6: a) Possible grip and b) Possible reverse grip

**Selection of possible grasp:** The selection of every possible grasp that can be performed on the object obeys a set of conditions set forth in steps 8-11 of the flowchart of Fig. 1. Each conditional applies to each of the cutouts (imcHB and imcHN) obtained in the “image path” section and only the cut that surpasses all the conditionals is considered as a possible grasp and is stored in a variable that contains all the possible grips. If the cut does not meet any of the conditionals it is discarded and the box is again moved to evaluate the grasp in a new position.

In step 8 is the first conditional which only searches for those cuts where there is no possibility of collision between the tips of the clamp and the object and for this it sums up the amount of white pixels in the first and last row of the imcHB cutout. If the sum is equal to zero, it means that all pixels are black and therefore, correspond to the background of the image but if the sum is different from zero, then there is some white pixel that corresponds to the object and implies a possible collision between the gripper and the element which is why the clipping is eliminated as a possible grasp.

In Eq. 1 the sum of all the pixels of the first and last row of the imcHB cutout with black background is represented where ReDim are the dimensions of the image and  $S_1$  is the result of the addition:

$$S_1 = \sum_{i=1}^{ReDim} imcHB(1, i) + imcHB(ReDim, i) \quad (1)$$

The first and last row of the imcHB cutout are marked with a box in Fig. 7c and correspond to the positions that would occupy the tips of the clamp in the work space. In Fig. 7a, there is the binary black input image imHB in Fig. 7b, it is the imHB image rotated with the box that is moving through the image, located on a possible grip and Fig. 7c shows the possible grip captured by the box.

In step 9 of the flowchart of Fig. 1, it is the next conditional that applies only if the cutout exceeds

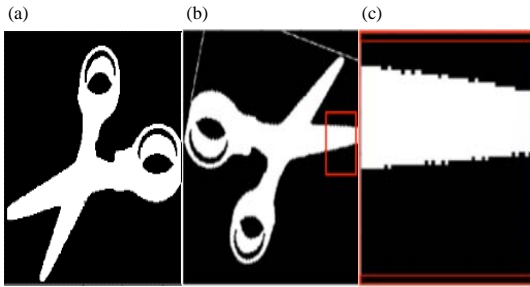


Fig. 7: Binarized image: a) ImHB; b) Rotated binarized image imHB and c) imcHB cutout as possible grasp

step 8. This conditional evaluates the thickness of the element where the grasp is sought in order to avoid considering as a possible grasp an image that contains only free pixels or noise or a very small gripping surface where there is a risk of the object falling or where the object is so thick that the fit between the gripper and the section of the object is too narrow. To determine which cutout meets this condition, all pixels of imcHB are summed in Eq. 2 and compared to a maximum and minimum value of white pixels that are calculated by Eq. 3-5.

In Eq. 3 it is determined the Maximum amount of white pixels (Max) in the imcHB cutout with respect to the total amount of Pixels in the cutout (Px) and a maximum Percentage of white (Pmax) while Eq. 4 determines the Minimum amount of white pixels (Min) in imcHB with respect to the total number of pixels in the cutout and a minimum percentage of white (Pmin):

$$S_2 = \sum_{i=1}^{Re\ Dim} \sum_{j=1}^{Re\ Dim} imcHB(i, j) \quad (2)$$

$$Max = Px \times Pmax \quad (3)$$

$$Min = Px \times Pmin \quad (4)$$

$$Px = B \times A \quad (5)$$

The total amount of pixels in the cutout is calculated as the multiplication between the dimensions A and B or aperture and width of the gripper as they are the same dimensions of the cutout.

If  $S_2$  is greater than min and less than max, the cut follows the conditional of step 10, otherwise it is discarded and returned to step 6 of Fig. 1 to move the box one position.

In step 10 of the flowchart of Fig. 1, the degree of inclination (inc) of the section of the object in the imcHB

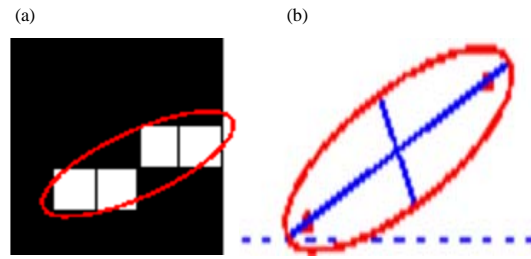


Fig. 8: Calculation of the inclination of the section of the object

cutout with respect to the surface of the gripper is evaluated. To obtain the degree of inclination (inc) an ellipse is drawn over the white pixels area of the imcHB cutout as shown in Fig. 8a and the ellipse's longest axis inclination with respect to the x-axis is calculated as shown in Fig. 8b.

In Fig. 8a, the white squares represent the pixels and the curved line, the ellipse that is drawn over the area. In Fig. 8b, the curved line is the ellipse drawn over the area of white pixels, the solid lines are the axes of the ellipse and the dotted line is the x-axis with respect to which the degree of inclination is measured.

The Maximum Incline value (IncMax) of the object with respect to the gripper is determined by the user and entered in degrees. The section of the object captured in the imcHB cutouts must have an inclination (inc) less than or equal to the maximum incline IncMax to overcome the condition of step 10. This criterion was added in order to control the maximum permissible slope between the object and the gripper as large inclination values can cause the object to move from its location and reduce grip accuracy while the gripper is closing.

In step 11 of the flowchart of Fig. 1, there is the last condition to be overcome by the cutout to be saved as a possible grasp. The criterion is to look for those cuts where there is a minimum amount of white pixels at the top and bottom edges of the imcHN cutout in order to accept only those that have enough space to fit the tips of the gripper into the grasp. Because dimension a considers not only the opening of the gripper but also the width of the tips it must be taken into account that part of the area of the cut imcHN includes the area occupied by the gripper in the space. In Fig. 9, it is possible to physically observe the dimensions that make up the crop box and the area occupied by the tips of the gripper.

The shaded section in Fig. 9 represents the thickness of the tips of the gripper which equates to the minimum amount of white pixels that must be inside the cutout to ensure that there is sufficient space for the gripper to fit the object.

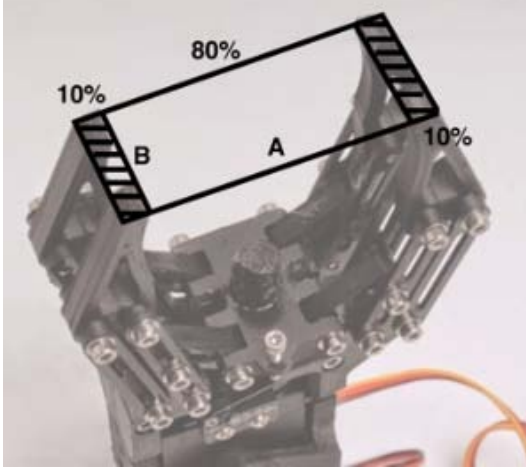


Fig. 9: Cutout dimensions and area of the gripper tips

To determine which cuts (imcHN) meet the last conditional, the number of top and bottom rows of the cutout that must have white pixels is defined, so that, the number of rows to be evaluated corresponds to the actual thickness of the gripper tips. As shown in Fig. 9, a Percentage (Pg) of the area occupied by each tip of the gripper is obtained with respect to the total area of the box, obtaining a  $Pg = 10\%$  for each tip and  $80\%$  of the free area for gripping the object. With the percentage Pg, the number of rows of pixels (fp) to be added to evaluate the conditional of step 11 is calculated. In Eq. 6, it is calculated the number of rows of pixels (fp) and in Eq. 7 the sum of pixels of the imcHN cutout in the upper and lower rows is performed:

$$fp = A \times Pg \quad (6)$$

$$S_3 = \sum_{i=1}^{fp} \sum_{j=1}^{ReDim} imcHN(i, j) + imcHN(ReDim - i + 1) \quad (7)$$

After obtaining the sum of  $S_3$  pixels, a comparison is made between  $S_3$  and the minimum amount of white Pixels (Pw) that must be at the ends of the cut-off multiplied by a noise factor wh between 0 and 1 that allows to consider the existence of very small areas of white pixels at the upper and lower edges of the cut where this factor is determined by the user according to the quality of the binarized image that is obtained after the segmentation.

In Eq. 8, the calculation of the minimum amount of white pixels that the cut at the upper and lower edges is to be taken according to the conditional of step 11 is

performed. The Percentage Pg is multiplied by two to obtain the total area occupied by both gripper tips in the box, the dimensions of the box (A and B) to have the total area and the noise factor wh:

$$Pw = 2 \times wh \times A \times B \times Pg \quad (8)$$

In step 12 of the flowchart of Fig. 1, all cuts that meet the conditionals in steps 8-11 are saved as possible grips. The imcHB cutout is stored in an IgHB variable, the coordinates of its upper left corner (x, y) in the Igx and Igy arrays, respectively the angle of inclination of the grip section with respect to the surface of the tips of the gripper (inc) in the IgAr array and the degree of rotation in which the binarized image (imHB and imHN) is located at the time of evaluating the cut is stored in the IgAh array.

In case the binarized image rotates  $180^\circ$  and when finished does not save any cut as possible grasp, the algorithm enters the conditional of step 13 and 14 to indicate that it did not find any grip zone and ends the process. Otherwise, enter the conditionals in steps 15-17 to choose a single grasp of all stored.

**Selection of the final grasp:** The first criterion of selection is focused on looking for the cut with the greatest grasp area and the lowest degree of inclination of the tool with respect to the gripper. To do this, in step 15 of Fig. 1, the 10 cuts with the largest grasp area are stored and then the one with the smallest inclination (inc) is selected.

To calculate the gripping area of each cut, all pixels of the cutout are added applying Eq. 2 and the 10 with the largest sum are chosen. Then, the degrees of inclination (saved in IgAr) of the 10 winning cuts are compared and the one with the lowest value is chosen without considering the sign. Finally, the position of the winning cut in the IgHB array is saved in iBest1.

The second selection criterion focuses on finding the grip having the largest contact surface between the object and the gripper in order to obtain the greatest friction between them. For this, in the step 16 of Fig. 1, the section of the object which more closely resembles a rectangle whose upper and lower edges are parallel to the surface of the tips of the clamp is sought for this the fit of the section of the captured object is evaluated in the cutout imcHB with respect to the lower edge of the cutout.

On the white pixels that are connected to each other and represent the object in the cutout imcHB, a rectangle is drawn that covers them completely (Fig. 10) with coordinates (X, Y) on the upper left corner and its width and height (X\_wigth, Y\_wigth, respectively).

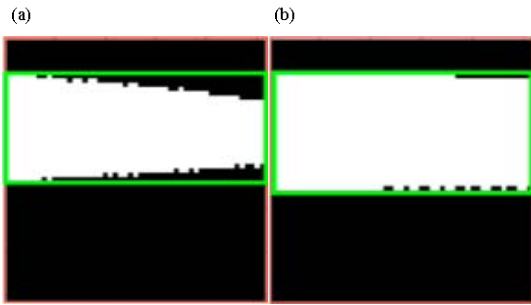


Fig. 10: Selection of the best fit

With the obtained dimensions of width and height of the rectangle its area is calculated and subtracted the total amount of white pixels (Eq. 2) of the corresponding cut in IgHB, so that, if the subtraction is equal to zero it means that the section of the object is completely rectangular and therefore has the best fit with the tips of the gripper, otherwise, it is assumed that the surface of the object is inclined or is irregular or has a curved geometry and therefore, there is not enough contact surface to make the grip.

Figure 10a shows the box covering the study of the object and the voids between the object and the box while Fig. 10b shows a more exact fit between the section of the object and the box. The winning cut between the two according to the criterion of step 16 would be that of Fig. 10b.

From all the stored cuts, the winning grasp is chosen when the subtraction between the area of the box and the total sum of its pixels S2 is minimal and its position in the arrangement is reserved in iBest2.

After obtaining the results iBest1 and iBest2, the algorithm proceeds to step 17 where it is chosen among the winning cuts which is closer to the centroid of the object to ensure a greater balance in the grasp.

First, the distance between the center of the winning cutouts and the centroid of the object is calculated, then choose the shortest distance of the two and save the result in iBest, so, if the largest area crop wins, iBest1 is saved to iBest, otherwise iBest2 is saved to iBest.

The side A of the rectangle of Fig. 11 represents the maximum aperture of the gripper or dimension A initialized in step 1 of Fig. 1 and the side B represents the thickness of the tips of the gripper or the dimension B initialized in step 1 of Fig. 1. The values of Xc were taken positive from the left edge of the image to the right and Yc positive from the upper edge of the image down. The angle of inclination Ang was taken with respect to the horizontal of the image and the horizontal of the cut as seen in Fig. 11.

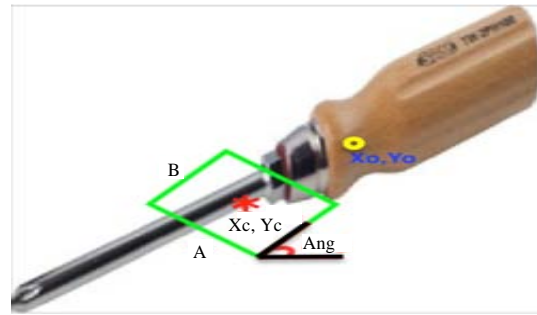


Fig. 11: Position and orientation of the gripper for the chosen grasp.  $X_c = 99$ ,  $Y_c = 145$ ,  $Ang = 50^\circ$ ,  $t = 1.723758$  sec

Table 1: Initialization of variables

Variables	Values
Pmax (%)	90
Pmin (%)	20
Grade (°)	5
Inc max (°)	15
Pg (%)	10
wh (%)	98

## RESULTS AND DISCUSSION

The algorithm developed was validated with several types of objects, different dimensions A and B of the gripper and with the initialization of variables set in Table 1.

**Initialization of variable:** The Pmax variable was chosen as 90% to allow fairly robust grip sections and Pmin as 20% both to avoid very thin grip sections and to filter false “possible grips” generated by white pixels that do not belong to the object.

The variable “Grade” indicates how many degrees the binarized image is rotated in steps 4 and 5 of Fig. 1 for the search of possible grips and was chosen as  $5^\circ$  to reduce the execution time of the algorithm without losing many possibilities of grasp. In a real application, this variable must be assigned with a value equal to or greater than the rotating resolution of the gripper, since, this will define the final degree of rotation of the gripper to make the grasp on the object.

The variable “IncMax” indicates the Maximum degree of Inclination of the grip section of the object with respect to the surface of the tips of the gripper. It was chosen as  $15^\circ$  in order to reduce the execution time of the program by filtering all other inclinations and to prevent the object from moving too much when the gripper fits over it as this can affect the grasp when generating a displacement in the object.



Fig. 12: Grasp point for open scissors;  $X_c = 33$ ,  $Y_c = 142$ ,  $Ang = 209$ ,  $t = 2.016619$  sec

The  $P_g$  variable was initialized to 10% assuming that each gripper tip do not occupy more than 10% of the total grip area and the percentage of acceptable noise  $wh$  was defined as 98% because the images used do not have much noise thanks to the white background.

**Results obtained:** The first test, illustrated in Fig. 12, yielded a grip section located on the cutting edge of the scissors for dimensions  $A = 60$  pixels and  $B = 50$  pixels. Under these measures the aperture was not sufficient to perform the grip on the tool handle, so, the only option that the algorithm found was the edge, a complicated position to handle for a gripper because of the thickness of the section of the object as well as its geometry its distance from the centroid and the care necessary for the cutting edge of the element. The computation time ( $t$ ) of the algorithm was 2.017 sec to calculate the grip and plot the results.

The geometry of the gripping section of Fig. 12 is inclined, so that, it can generate slip between the gripper and the object and cause the scissors to fall as well as the distance between the grip and the centroid that can cause the weight of the scissors to affect the stability of the grasp.

Due to the results obtained in the first test, the dimensions of the box were changed by  $A = 50$  pixels and  $B = 30$  pixels obtaining the results of Fig. 13. In this case, the grasp that was selected by the algorithm is located closer to the centroid of the tool and is located on the handle of the scissors. Compared to the previous test, the chances of the object slipping due to the grip geometry are reduced, since, both the handle and the scissors top have a larger area than the shaft where the grasp is made and there is no risk of damaging the quality of the cutting



Fig. 13: Grasp point for open scissors with narrower gripper;  $X_c = 109$ ,  $Y_c = 96$ ,  $Ang = 852$ ,  $t = 1.850442$  sec



Fig. 14: Grasp point for closed scissors;  $X_c = 86$ ,  $Y_c = 111$ ,  $Ang = 02$ ,  $t = 1.779819$  sec

edge. The disadvantage with the grasp of Fig. 13 is that the location of the gripper on the tool must be very precise, so that, the gripper engages in the middle of the handle of the scissors without touching it.

For a second test with  $A = 60$  pixels and  $B = 50$  pixels, closed scissors were used as in Fig. 14 where the winning grasp was placed on the scissors, almost on the screw as close as possible to the centroid without having to be placed on the handle. This grasp does not affect the cutting edge of the tool but as in the first test, the object may slip due to the geometry of the grip section. To ensure a stable fastening in the position of the box of Fig. 14 it is required that the surface of the gripper has a high level of friction with the surface of the object and that it exerts sufficient force both to lift the object and to prevent it from tilting due to pressure.

The dimensions of the box were changed to look for another grasp point, obtaining the result of Fig. 15 for  $A = 50$  pixels and  $B = 30$  pixels. The section of the object





Fig. 15: Grasp point for closed scissors with a narrower gripper;  $X_c = 185$ ,  $Y_c = 182$ ,  $Ang = 1102$ ,  $t = 2.003006$  sec

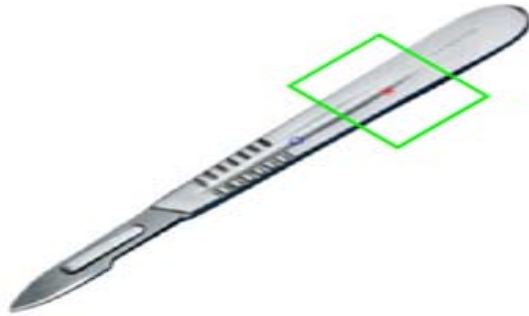


Fig. 16: Grasp point for a scalpel;  $X_c = 159$ ,  $Y_c = 66$ ,  $Ang = 459$ ,  $t = 1.965278$  sec

chosen for the grip was found on the handle where the advantage of this grasp is that if the tool is tilted or slid slightly can be pinned to the gripper as the gripper encloses the entire handle.

For the first two tests it is concluded that the best grasp is the one that is placed on the handle of the scissors, since, it is less likely to slip and the geometry of the scissors makes the grasp more stable for the reasons already mentioned. However, to achieve the grasp chosen by the algorithm on the handle it is necessary to handle a high precision in the location of the gripper, since, one of the tips of the gripper must fit in a space with reduced area as observed in the Fig. 13 and 15.

In a third test, the grasp points were located on a surgical scalpel obtaining the results shown in Fig. 16 for dimensions  $A = 60$  pixels and  $B = 50$  pixels and in Fig. 17 for dimensions  $A = 50$  pixels and  $B = 30$  pixels. Because the scalpel's geometry is not as irregular as that of the scissors, any possible grasp is placed on its body and differ from each other by the distance between the grasp and the centroid of the tool where the difference of the



Fig. 17: Grasp point for a scalpel with a narrower gripper;  $X_c = 128$ ,  $Y_c = 105$ ,  $Ang = 459$ ,  $t = 2.119956$  sec

grasp for both cases lies in the application of the conditionals of the steps 15 and 16 of Fig. 1 and the choice of the final grasp in step 17.

From the tests performed it is possible to observe that, depending on the dimensions of the gripper that is handled in the application, different grasp points can be obtained for the same object. On the other hand, the quality of the grasp depends on the conditionals of steps 15 and 16 of Fig. 1, since, they define which the two best grips are and then the winner is chosen.

The distance between the grasp and the centroid is important to find stable grips, however, for the object presented its relevance appeared after having chosen two possible grips. This is because the centroid obtained in the algorithm is based on the geometry of the object but not on its weight, so, in cases where the center of mass and the centroid of the object differ considerably, a grasp on the centroid cannot ensure a stable grip which is why the conditionals of steps 15 and 16 were established to try to set grips that consider mass changes in different areas of the object.

In Fig. 18 different grasp positions can be observed for various types of elements with slight variations in the variables of Table 1 and the dimensions of the crop box,  $A$  and  $B$ . In the upper part of each image, the values of the variables that were changed with respect to Table 1 are defined and in the lower part the runtime results of the algorithm ( $t$ ) from step 1 of Fig. 1 to step 19, the total number of possible grips found ( $n$ ) and winning selection criterion ( $g$ ) between "Greater area" for the conditional of step 15 of Fig. 1 and "Best fit" for the conditional of step 16.

**Efficient rotation range for grasp detection:** In this validation two tools with different geometries were taken and points of grab were sought on each of them, varying the value of "Grade" between  $1$  and  $90^\circ$  as shown in Table 2 and 3 in order to determine the efficient rotation

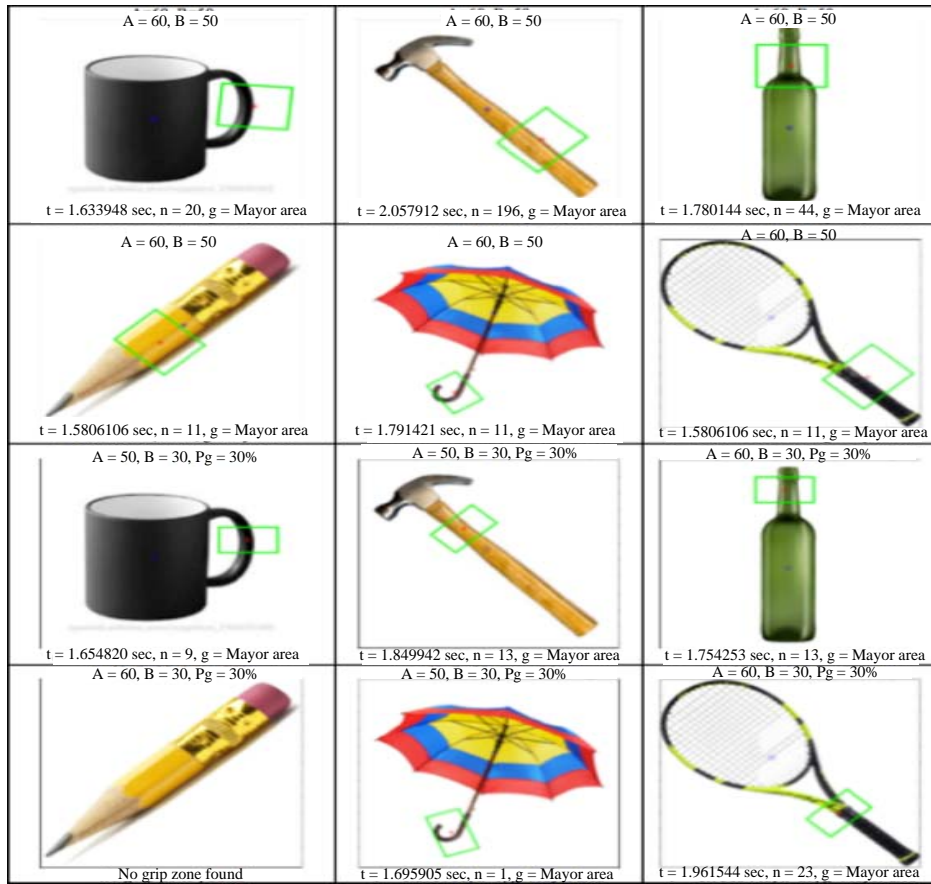


Fig. 18: Grasp points obtained for different elements

Table 2: Results of the selection of grip for curved scissors

Objects/Grade (°)	Time (sec)	Distance for largest area (pixels)	Distance for best fit (pixels)	g	n	Distance (pixels)
<b>Curved scissors</b>						
1	8.52582	51	85	Largest area	260	51
2	4.26537	50	95	Largest area	125	50
3	2.83418	72	85	Largest area	86	72
4	2.36687	50	76	Largest area	68	50
5	1.87705	154	85	Best fit	56	85
6	1.58548	158	88	Best fit	50	88
7	1.42399	150	85	Best fit	30	85
8	1.34685	158	76	Best fit	41	76
9	1.08287	51	76	Largest area	32	51
10	1.0022	118	75	Best fit	24	75
20	0.54706	118	92	Best fit	12	92
30	0.41208	149	92	Best fit	13	92
40	0.37781	96	92	Best fit	6	92
50	0.41179	103	80	Best fit	10	80
60	0.27439	96	92	Best fit	6	92
70	0.44958	118	100	Best fit	3	100
80	Not found	-	-	-	-	-
90	Not found	-	-	-	-	-

range of the image in steps 4 and 5 of Fig. 1, allowing a final grasp on the object to be selected in the shortest possible time.

In the tests the same values of Table 1 were used, except for the grade variable. Fixed values were defined

for the dimensions A and B of the box equal to 50 pixels and 30 pixels, respectively and the results obtained were plotted.

Table 2 and 3 recorded the execution time of the algorithm for each value of “Grade” in seconds (time), the

Table 3: Results of the grasp selection for grippers

Objects/Grade (°)	Time (sec)	Distance for largest area (pixels)	Distance for best fit (pixels)	g	n	Distance (pixels)
<b>Clamp</b>						
1	9.21838	110	48	Best fit	794	48
2	5.07955	113	38	Best fit	397	38
3	3.43495	113	38	Best fit	262	38
4	2.66762	113	38	Best fit	197	38
5	2.02961	47	38	Best fit	157	38
10	1.12405	222	48	Best fit	75	48
20	0.61474	222	30	Best fit	42	30
30	0.44984	179	118	Best fit	10	118
40	0.46384	222	30	Best fit	21	30
50	0.33584	179	16	Best fit	17	16
60	0.23372	98	118	Largest area	4	98
70	0.35437	118	22	Best fit	24	22
80	0.17025	98	118	Largest area	4	98
90	0.35725	98	118	Largest area	4	98



Fig. 19: No grip zone was found

distance between the chosen grasp in the conditional of step 15 of the flowchart of Fig. 1 and the centroid of the object (distance for largest area), the distance between the chosen grasp in the conditional of step 16 of the flowchart of Fig. 1 and the centroid of the object (distance for best fit), the winning selection criterion (g), the total number of possible grips found (n) and the distance between the final grasp and the centroid of the object (distance).

The scissors selected for the tests in Table 2 are those shown in Fig. 19 and 20 where five of the tests performed on the tool were drawn.

In Table 2, it can be observed that the algorithm was able to select grasp positions in the tool for degrees of rotation up to 70°, reaching a maximum of 260 possible grasp positions when rotating the tool one degree in each iteration and up to 3 possible grips for rotations every 60°. In Fig. 1, they were plotted the values obtained for the total number of possible grips (n) with circular symbols,

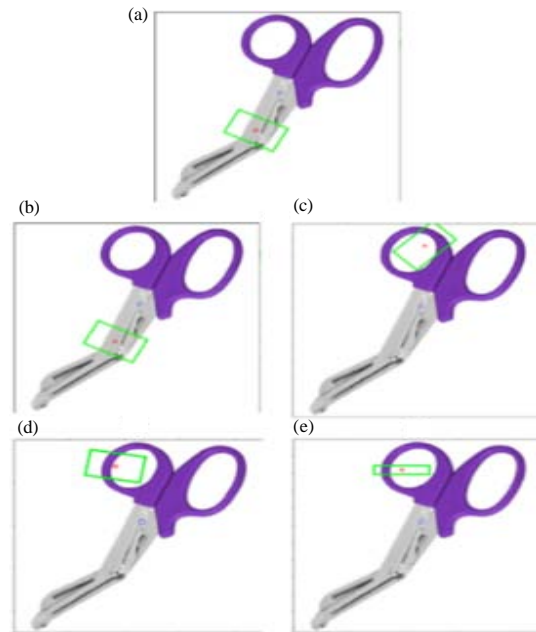


Fig. 20: Tests made for curved scissors with grade equal to; a) 1°; b) 4°; c) 45°; d) 70° and e) y 90°

the distance between the winning grasp and the centroid of the tool with triangular symbols and the execution time of the algorithm with square symbols, all with respect to the degree of rotation “Grade”.

The execution time of the algorithm is extremely high for grade values <5° due to the high amount of “possible grips” that the algorithm must evaluate to choose the final grasp, reaching an execution time of up to 8.5 sec to evaluate 260 grasp positions, most of which are too close to each other. As can be seen in Fig. 20 for rotations <10°, the final grasp was placed in the same position as that obtained with grade = 1° and in less than half the time. Figure 20a shows the grasp selection for grade = 1° and Fig. 20b shows the grasp for grade = 4°.

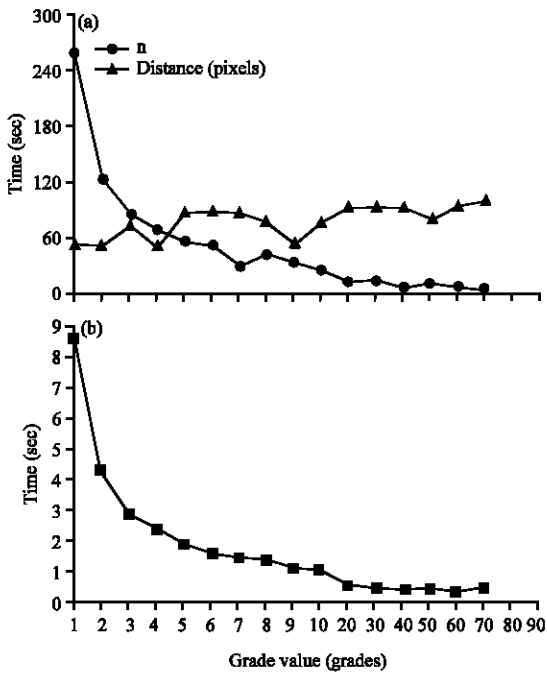


Fig. 21: a, b) Graph the results for the grasp of curved scissors

On the other hand, the reduction in execution time begins to stabilize after 20° where a time of about half a second is reached with <15 possible grips to evaluate but with grip distances farther from the centroid. After 20°, the number of possible grips is reduced and it starts to oscillate between 15 and 3 grips according to the value of grade.

Figure 20c and d show possible grips calculated with angle criteria above 20° where the free grip area required by the gripper to be able to grip the object at the desired point becomes narrower but is placed correctly in the handle of the scissors. In Fig. 20e, the dimensions of the gripper were changed to look for possible grips with a grade value higher than 70°, finding that for A = 50 pixels and B = 10 pixels, the algorithm succeeds in finding a gripping section that meets the conditions of steps 8-11 of Fig. 1 on one of the scissor finger holes.

Figure 21 shows a significant decrease between program execution times and the value of n for grade values between 1 and 3°, almost halving as it increases by one to the degree of rotation. After 3° the decrease of the time and of n stops being elevated and the change stops to be noticed around the 6°.

The pliers selected for the tests in Table 3 are those shown in Fig. 22 where five of the tests performed on the tool are presented.

In Table 3, in comparison to Table 2, the algorithm was able to select grasp positions in the tool for degrees of rotation up to 90°, reaching a maximum of 794 possible

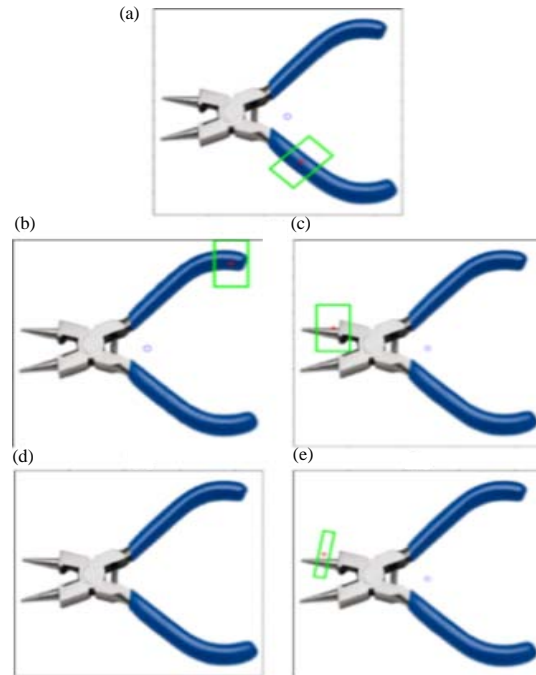


Fig. 22: Tests performed for the pliers with grade equal to; a) 5°; b) 30°; c) 60°; d) 60° with A = 50 pixels and B = 10 pixels; (e) y 10° with A = 50 pixels y B = 10 pixels

grasp positions when rotating the tool one degree at each iteration and up to 4 possible grips for rotations every 90°. Figure 22 illustrates the values obtained for the total number of possible grips (n) with circular symbols, the distance between the winning grasp and the centroid of the tool with triangular symbols and the execution time of the algorithm with square symbols, all with respect to the degree of rotation “Grade”.

As in Fig. 23, there were high execution times for small values of “Grade” reaching to exceed 9 sec in grade = 1°. Simultaneously, time and n reductions of about half the previous value were observed between the first three degrees. Around 5° the algorithm achieved an execution time of 2 sec, very close to the execution time of the scissors. From the 10° onwards, the behavior of time came much closer to that of Fig. 21, stabilizing after the 20° as well as the number of possible grips n which ranges from 30-4 possible grips.

Figure 22a shows the grasp selection for grade = 5°, Fig. 22b shows the grasp for grade = 30° and Fig. 22c shows the grasp for grade = 60°. In all three cases, different grasp points were obtained where the most stable was found with grade = 5° while the others were positioned near the ends of the tool where the object could fall.

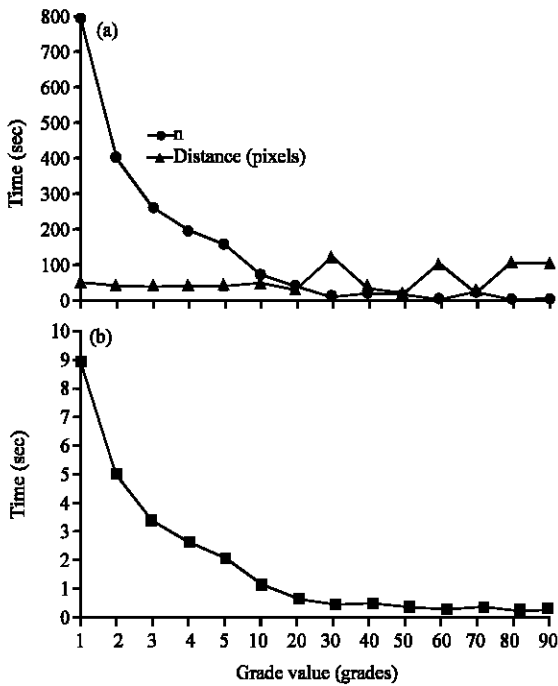


Fig. 23: a, b) Graph of the results for the grasp of the gripper

On the other hand, in Fig. 22d and e the dimensions of the gripper were changed by  $A = 50$  pixels and  $B = 10$  pixels, obtaining a considerable change in the selection of the grasp where the algorithm failed to find any grasp for a grade =  $60^\circ$  after finding 4 possible grips for this value of rotation with the dimensions  $A = 50$  pixels and  $B = 30$  pixels of the box and found a grasp for  $10^\circ$  much farther than that obtained with the previous dimensions of the gripper, reaching to position almost in the same location as the centroid found in Fig. 22c for  $60^\circ$ .

**Analysis of results:** According to the requirements of the application where the algorithm is executed, grade values below  $10^\circ$  can be used to evaluate several grasp points and have a final grasp near the centroid with a minimum execution time of 1 sec and a maximum of 9 sec or search for grips quickly with grade values between 10 and  $20^\circ$  to achieve a minimum execution time of almost 500ms and distances near the centroid. Using a grade value greater than or equal to  $30^\circ$  does not significantly improve grasp selection or run time, so that, angles above this value only reduce the amount of possible grips, discarding those that could generate a good grasp.

As noted in Fig. 20 and 22, grasp selection depends on the “Grade” value and the A and B dimensions of the crop frame because it defines the gap occupied by the gripper in the work area and on it depends the space that

Table 4: Reduction of the number of possible grasp

Grade ( $^\circ$ )	n-test	n-Calculated	Relative error (%)	Average(%)
1	794	794.00	0.00	2.030
2	397	394.00	0.00	-
3	262	264.67	1.01	-
4	197	198.50	0.76	-
5	157	158.80	1.13	-
10	75	79.40	5.54	-
20	42	39.70	5.79	43.20
30	10	26.47	62.22	-
40	21	19.85	5.79	-
50	17	15.88	7.05	-
60	4	13.23	69.77	-
70	24	11.34	111.59	-
80	4	9.93	59.70	-
90	4	8.82	54.66	-

will require the gripper to be able to perform the grasp. On the other hand, the geometry of the object also influences the selection of the grasp, since, the object can have many possibilities of grasp, e.g., the curved scissors or a single gripping section as in the case of the scalpel of Fig. 16.

When comparing the results of Table 2 and 3, it was observed that up to  $20^\circ$  the number of possible grips (n) for each degree of rotation (Grade) is approximately equal to the total amount of possible grips obtained with grade =  $1^\circ$  ( $n_1$ ) divided by the value of the degree of rotation of the image as shown in Eq. 9.

In Eq. 10 the relative error is calculated where ER is the Relative Error, n calculated is the number of possible grips calculated for grade and n-test is the amount of possible grips obtained in the tests:

$$n_{\text{Calculated}} \approx \frac{n_1}{\text{Grade}} \quad (9)$$

$$E_R = \left| \frac{n_{\text{Test}} - n_{\text{Calculated}}}{n_{\text{Calculated}}} \right| \times 100\% \quad (10)$$

After  $20^\circ$ , the value of n begins to decrease markedly away from the results of Eq. 9 as seen in Table 4 where the relative error for the pliers of Fig. 22, calculated with Eq. 9 is <6% for grade values between 1 and  $20^\circ$  and for values  $>30^\circ$ , ranges from 6-70% where the relative error for  $70^\circ$  is a particular case for the pliers due to their geometry.

The average between the relative errors (average) for “Grade”  $\geq 20^\circ$  was about 2% while for “Grade”  $\leq 30^\circ$  was almost 44% without considering the relative error of  $70^\circ$ . These results demonstrate that the amount of possible grips becomes very imprecise as the degree of rotation “Grade” increases.

## CONCLUSION

The established grasp criteria provided the algorithm with the parameters needed to select the one that would be considered the best grasp but in turn caused the selected grasp to move away from the centroid of the object by looking for a larger grip area which may be against the stability of the object upon being lifted. However, the centroid obtained does not consider the weight distribution of the element but only its geometry so it is not possible to guarantee that any position of grasp that is located on the geometric centroid of the object is stable, reason why it was preferred to choose the gripping section with greater contact surface to increase the friction between the gripper and the object. The search for stable grasp points for objects with geometric centroid different from the center of mass becomes part of a future research.

The execution time of the algorithm depends on the minimum rotation value in each iteration, the object geometry and the number of possible grips that exceed the conditionals in steps 8-11. A high number of possible grips does not mean an improvement in the quality of the final grasp, since, as it could be observed, the algorithm is able to recognize a few grasp points, selecting the same one that was found for small values of "Grade".

The selection of a "Grade" value that allows to find possible grips on almost any geometry of the entrance object, must be selected in values inferior or equal to  $20^\circ$  where it is possible to obtain up to a twentieth part of the total number of grasp points for grade =  $1^\circ$  independent of the geometry or location of the object in space while higher values will depend on the object and may not always work for any element as it was observed when comparing Table 2 and 3 for values  $>70^\circ$ .

Values equal to or above  $30^\circ$  allow different grasp points to be found on the object, however, there are no significant improvements in execution time with respect to  $20^\circ$  and the reduction of possible grasp points is imprecise as illustrated in Table 4, so, it is not advisable to use values  $>20^\circ$  for grade.

The high execution time of the algorithm obtained for small values of Grade is not justified, since, the results found with slightly higher values are very close or equal to the results of grade =  $1^\circ$  and it uses less than half the time, so, it is more efficient to use values between  $5^\circ$  and  $20^\circ$  where the maximum execution time is about 2 sec and the minimum about 500 msec.

## ACKNOWLEDGEMENT

Researchers are grateful to the Nueva Granada Military University which through its Vice Chancellor for research, finances the present project with code IMP-ING-2290 and titled "Prototype of Robot Assistance for Surgery" from which the present research is derived.

## REFERENCES

- Fernandez, C., M.A. Vicente, C. Perez, L. Jimenez and L. Paya, 2003. [Teleoperation learning: Application to the object-grabbing processes]. *Web Syst. Eng. Autom.* Alicante, 1: 18-19.
- Gualtieri, M., A.T. Pas, K. Saenko and R. Platt, 2016. High precision grasp pose detection in dense clutter. *Proceedings of the 2016 IEEE-RSJ International Conference on Intelligent Robots and Systems (IROS'16)*, October 9-14, 2016, IEEE, Daejeon, South Korea, ISBN:978-1-5090-3763-6, pp: 598-605.
- Jain, S. and B. Argall, 2016. Grasp detection for assistive robotic manipulation. *Proceedings of the 2016 IEEE International Conference on Robotics and Automation (ICRA'16)*, May 16-21, 2016, IEEE, Stockholm, Sweden, ISBN:978-1-4673-8026-3, pp: 2015-2021.
- Martin, J., 2015. [Algorithm of stumble (grip) depending on the tool for the robot arm IRB 120]. MSc Thesis, University of Alcala, Madrid, Spain. (In Spanish)
- Redmon, J. and A. Angelova, 2015. Real-time grasp detection using convolutional neural networks. *Proceedings of the 2015 IEEE International Conference on Robotics and Automation (ICRA'15)*, May 26-30 2015, IEEE, Seattle, Washington, ISBN:978-1-4799-6924-1, pp: 1316-1322.
- Sun, C., Y. Yu, H. Liu and J. Gu, 2015. Robotic grasp detection using extreme learning machine. *Proceedings of the 2015 IEEE International Conference on Robotics and Biomimetics (ROBIO'15)*, December 6-9, 2015, IEEE, Zhuhai, China, ISBN:978-1-4673-9675-2, pp: 1115-1120.
- Trottier, L., P. Giguere and B. Chaib-Draa, 2016. Dictionary learning for robotic grasp recognition and detection. *J. Eng. Appl. Sci.*, 1: 1-19.
- Wang, Z., Z. Li, B. Wang and H. Liu, 2016. Robot grasp detection using multimodal deep convolutional neural networks. *Adv. Mech. Eng.*, Vol. 8,
- Yon, 2016. [Algorithm for handling objects in a robot PR]. Msc Thesis, University of Chile, Santiago, Chile. (In Spanish).